

# A coherent study of $e^+e^- \rightarrow \omega\pi^0$ , $\omega\pi^+\pi^-$ , and $\omega\eta$

Yan Wu<sup>1,2</sup>, Qinsong Zhou<sup>3,4</sup>, Wenbiao Yan<sup>1,2</sup> , and Guangshun Huang<sup>1,2</sup>

<sup>1</sup>Department of Modern Physics, University of Science and Technology of China, Hefei 230026, China;

<sup>2</sup>State Key Laboratory of Particle Detection and Electronics, University of Science and Technology of China, Hefei 230026, China;

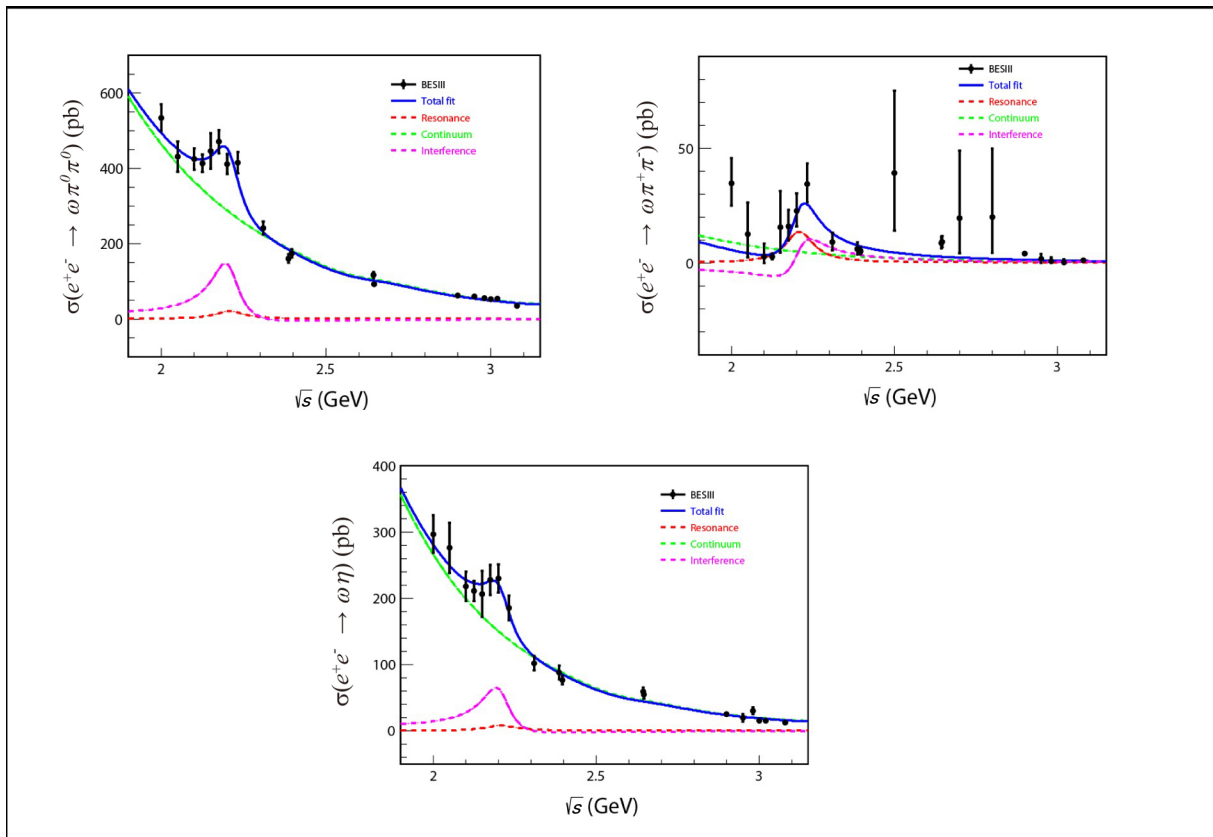
<sup>3</sup>School of Physical Science and Technology, Lanzhou University, Lanzhou 730000, China;

<sup>4</sup>Research Center for Hadron and CSR Physics, Lanzhou University & Institute of Modern Physics of CAS, Lanzhou 730000, China

Correspondence: Wenbiao Yan, E-mail: [wenbiao@ustc.edu.cn](mailto:wenbiao@ustc.edu.cn)

© 2023 The Author(s). This is an open access article under the CC BY-NC-ND 4.0 license (<http://creativecommons.org/licenses/by-nc-nd/4.0/>).

## Graphical abstract




Simultaneous fit of  $e^+e^- \rightarrow \omega\pi^0\pi^0$ ,  $\omega\pi^+\pi^-$ , and  $\omega\eta$  with one resonance.

## Public summary

- We perform a combined analysis on  $e^+e^- \rightarrow \omega\pi^0\pi^0$ ,  $e^+e^- \rightarrow \omega\pi^+\pi^-$ , and  $e^+e^- \rightarrow \omega\eta$  to study possible  $\omega$  excited states around 2.2 GeV.
- In the fit with one resonance, the mass and width are consistent with previous measurements.
- In the fit with two resonances, the masses and widths are consistent with theoretical predictions.
- The fitting result of  $\Gamma_R^{e^+e^-} B_R$  is partially consistent with experimental result and theoretical prediction.

# A coherent study of $e^+e^- \rightarrow \omega\pi^0$ , $\omega\pi^+\pi^-$ , and $\omega\eta$


Yan Wu<sup>1,2</sup>, Qinsong Zhou<sup>3,4</sup>, Wenbiao Yan<sup>1,2</sup> , and Guangshun Huang<sup>1,2</sup>

<sup>1</sup>Department of Modern Physics, University of Science and Technology of China, Hefei 230026, China;

<sup>2</sup>State Key Laboratory of Particle Detection and Electronics, University of Science and Technology of China, Hefei 230026, China;

<sup>3</sup>School of Physical Science and Technology, Lanzhou University, Lanzhou 730000, China;

<sup>4</sup>Research Center for Hadron and CSR Physics, Lanzhou University & Institute of Modern Physics of CAS, Lanzhou 730000, China

 Correspondence: Wenbiao Yan, E-mail: [wenbiao@ustc.edu.cn](mailto:wenbiao@ustc.edu.cn)

© 2023 The Author(s). This is an open access article under the CC BY-NC-ND 4.0 license (<http://creativecommons.org/licenses/by-nc-nd/4.0/>).



Cite This: *JUSTC*, 2023, 53(7): 0704 (9pp)



Read Online

**Abstract:** In this work, a combined analysis is performed on the processes of  $e^+e^- \rightarrow \omega\pi^0\pi^0$ ,  $e^+e^- \rightarrow \omega\pi^+\pi^-$ , and  $e^+e^- \rightarrow \omega\eta$  to study possible  $\omega$  excited states at approximately 2.2 GeV. The resonance parameters are extracted by simultaneous fits of the Born cross section line shapes of these processes. In the fit with one resonance, the mass and width are fitted to be  $(2207 \pm 14)$  MeV/ $c^2$  and  $(104 \pm 16)$  MeV, respectively. The result is consistent with previous measurements. In the fit with two resonances, the mass and width for the first resonance are fitted to be  $(2160 \pm 36)$  MeV/ $c^2$  (solution I),  $(2154 \pm 12)$  MeV/ $c^2$  (solution II) and  $(141 \pm 74)$  MeV (solution I),  $(152 \pm 77)$  MeV (solution II), respectively. The mass and width for the second resonance are fitted to be  $(2298 \pm 19)$  MeV/ $c^2$  (solution I),  $(2309 \pm 6)$  MeV/ $c^2$  (solution II) and  $(106 \pm 77)$  MeV (solution I),  $(99 \pm 23)$  MeV (solution II), respectively. The result is consistent with the theoretical prediction of  $\omega(4S)$  and  $\omega(3D)$ . The intermediate subprocesses in  $e^+e^- \rightarrow \omega\pi^+\pi^-$  are analyzed using the resonance parameters of the previous fits in this work. In the fit with one resonance, the fitting result of  $\Gamma_R^{e^+e^-} B_R$  is partially consistent with the previous result. In the fit with two resonances, the fitting result of  $\Gamma_R^{e^+e^-} B_R$  is of the same order of magnitude as the theoretical prediction. This work may provide useful information for studying the light flavor vector meson family.

**Keywords:**  $\omega$  excited states; simultaneous fit; light flavor vector meson

**CLC number:** O572.22

**Document code:** A

## 1 Introduction

In the low energy region, the nonperturbative effect of quantum chromodynamics (QCD) makes it difficult to calculate strong interaction processes precisely. Meanwhile, this effect influences almost all the nature of hadrons, including mass, decay, and production.

The study of light flavor mesons is one of the ideal approaches to understand nonperturbative QCD. In experiments, light flavor mesons could be studied by electron-positron collision and the process of a meson or photon scattering with a nucleon.

In electron-positron collisions, light flavor vector mesons can be abundantly produced, so the electron-positron collision experiment is an ideal platform to study vector mesons and the nature of strong interaction. After decades of effort, the spectroscopy of light flavor vector mesons below 1.8 GeV has been well established. However, in the energy region around 2–3 GeV, the study is insufficient. According to an unquenched relativized potential model<sup>[1–7]</sup>, there are many light flavor vector meson states around 2 GeV, and the energy gaps between them are very small. After taking the interference effect into consideration, it is difficult to measure their resonance parameters in an experiment, and the theoretical prediction of these states also needs to be more precise. Therefore, more study of these states around 2 GeV is needed. In this paper, we focus on the  $\omega$  excited states.

In the PDG (partial data group), there are seven  $\omega$  states<sup>[8]</sup>. The ground state is  $\omega(782)$ , which is a  $1^3S_1$  state.  $\omega(1420)$  and  $\omega(1960)$  are  $2^3S_1$  and  $3^3S_1$  states, respectively, and they are the first and second radial excited states of  $\omega(782)$ .  $\omega(1650)$  is a  $1^3D_1$  state<sup>[9–13]</sup>. The other states are in 2–3 GeV, including  $\omega(2205)$ <sup>[14]</sup>,  $\omega(2290)$ <sup>[15]</sup>, and  $\omega(2330)$ <sup>[16]</sup>.  $\omega(2205)$  and  $\omega(2290)$  are observed in  $p\bar{p}$  collision experiments, and  $\omega(2330)$  is observed in  $\gamma p \rightarrow \rho^+\rho^0\pi^+$ . According to the Regge trajectory analysis<sup>[9]</sup>,  $\omega(2205)$  may be the second radial excited state of  $\omega(1650)$ , which is a  $3^3D_1$  state.  $\omega(2290)$  and  $\omega(2330)$  may be the third radial excited states of  $\omega(782)$ , which are  $4^3S_1$  states. So far, the BABAR and BESIII collaboration have reported some measurement results of the relevant resonances<sup>[17–22]</sup>. Assuming they are  $\omega$  excited states, their widths are significantly smaller than PDG values<sup>[8]</sup> and theoretical prediction<sup>[9]</sup>, which raises doubts about these results. Fig. 1 shows the comparison of the resonance parameters of these reported states.

Among these measurements, the BESIII results of  $e^+e^- \rightarrow \omega\pi^0\pi^0$ <sup>[21]</sup>,  $e^+e^- \rightarrow \omega\pi^+\pi^-$ <sup>[20]</sup>, and  $e^+e^- \rightarrow \omega\eta$ <sup>[22]</sup> are very useful for studying  $\omega$  excited states. Three enhancement structures around 2.2 GeV are observed in these processes. Their masses and widths are  $M_1 = (2222 \pm 7 \pm 2)$  MeV/ $c^2$ ,  $\Gamma_1 = (59 \pm 30 \pm 6)$  MeV,  $M_2 = (2250 \pm 25 \pm 27)$  MeV/ $c^2$ ,  $\Gamma_2 = (125 \pm 43 \pm 15)$  MeV, and  $M_3 = (2179 \pm 21 \pm 3)$  MeV/ $c^2$ ,  $\Gamma_3 = (89 \pm 28 \pm 5)$  MeV, respectively. All of them are possible  $\omega$  excited states. The resonance parameters are

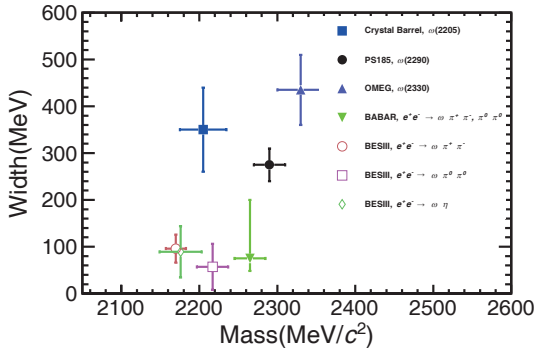


**Fig. 1.** A comparison of resonance parameters of these reported  $\omega$  states with masses around 2.2 GeV<sup>[14–22]</sup>.

obviously different from each other, and they are inconsistent with the PDG values. According to the previous theoretical analysis of  $e^+e^- \rightarrow \omega\pi^0\pi^0$  and  $\omega\eta$ <sup>[23]</sup>, the resonances are contributed by  $\omega(4S)$  and  $\omega(3D)$ . While in  $e^+e^- \rightarrow \omega\eta$ , the  $\omega(4S)$  is dominant, and in  $e^+e^- \rightarrow \omega\pi^0\pi^0$ , the contributions from  $\omega(4S)$  and  $\omega(3D)$  are similar. The difference in their resonance parameters originates from the different contributions of  $\omega(4S)$  and  $\omega(3D)$  and the interference between these two states. In this paper, with additional data from  $e^+e^- \rightarrow \omega\pi^+\pi^-$ , we perform a further analysis that can verify the previous conclusion and provide more information on the  $\omega$  meson family in 2–3 GeV.

The analysis is carried out with the following parts. First, by assuming that the resonances observed in these processes are the same, a simultaneous fit is performed in Section 2. Then, an additional fit is performed by inputting two resonances standing for  $\omega(4S)$  and  $\omega(3D)$ , which is in Section 3. In Section 4, the intermediate processes in  $e^+e^- \rightarrow \omega\pi^+\pi^-$  are analyzed with two simultaneous fits and the input of the resonance parameters obtained before. Conclusions are in Section 5.

## 2 Simultaneous fit of the three processes

According to the constraint from symmetry and the Okubo-Zweig-Iizuka (OZI) rule, the resonances observed in  $e^+e^- \rightarrow \omega\pi^0\pi^0, \pi^+\pi^-$ , and  $\omega\eta$  are all possible  $\omega$  excited states. However, it is difficult to distinguish what exactly these states are due to a lack of precision. Therefore, we assume these resonances are the same and perform a simultaneous fit.

### 2.1 Fitting method

To describe the Born cross section line shapes of the three processes and extract the resonance parameters, a minimized  $\chi^2$  fit is performed on the cross sections. The  $\chi^2$  is defined by

$$\chi^2 = \sum_{\sqrt{s}} \Sigma^T V^{-1} \Sigma, \quad (1)$$

$\Sigma^T$  is defined by

$$\Sigma^T = (\sigma_1^{\text{exp}} - \sigma_1^{\text{fit}}, \sigma_2^{\text{exp}} - \sigma_2^{\text{fit}}, \sigma_3^{\text{exp}} - \sigma_3^{\text{fit}}), \quad (2)$$

where 1, 2, and 3 stand for  $\omega\pi^0\pi^0, \omega\pi^+\pi^-$ , and  $\omega\eta$  modes, respectively.  $V$  is the covariance matrix, whose element  $V_{i,j}$  is defined as

$$V_{i,j} = \sum_k x_i \times \epsilon_{i,j,k} \times x_j \times \epsilon_{j,i,k}, \quad (3)$$

where  $x_{i,j}$  is the measured cross section value at energy point  $(i, j)$ ,  $\epsilon_{i,j,k}$  is the common uncorrelated uncertainty of  $x_i$  and  $x_j$  from correlated source  $k$ . There is no correlated uncertainty.

The total fitting function is a coherent sum of resonant and non-resonant contributions:

$$\sigma^B(\sqrt{s}) = |A_r(\sqrt{s})e^{i\phi} + A_c(\sqrt{s})|^2, \quad (4)$$

where  $\phi$  is the relative phase between the resonant and non-resonant amplitudes,  $A_r(\sqrt{s})$  is the resonant component, which is parameterized with a Breit-Wigner function as:

$$A_r(\sqrt{s}) = \frac{M_R}{\sqrt{s}} \frac{\sqrt{12\pi C \Gamma_R^{e^+e^-} B_R \Gamma_R}}{s - M_R^2 + iM_R \Gamma_R} \sqrt{\frac{P(\sqrt{s})}{P(M_R)}}, \quad (5)$$

where  $M_R$  and  $\Gamma_R$  are the mass and width of the resonant structure, respectively.  $\Gamma_R^{e^+e^-} B_R$  is the product of the electronic width of the resonance  $R$  and the branching fraction of the decay of the resonance to the final state.  $C$  is a constant that equals to  $3.893 \times 10^5 \text{ nb} \cdot \text{GeV}^{2[17]}$ .  $P(\sqrt{s})$  is the two- or three-body phase space factor. The non-resonant component  $A_c(\sqrt{s})$  is parameterized as:

$$A_c(\sqrt{s}) = \frac{a \sqrt{P(\sqrt{s})}}{\sqrt{s}^b}, \quad (6)$$

where  $a$  and  $b$  are free parameters. In the simultaneous fit,  $M_R$  and  $\Gamma_R$  are shared parameters, so there are 14 free parameters in total, including  $M_R, \Gamma_R$ , and three sets of  $\phi, \Gamma_R^{e^+e^-} B_R, a$ , and  $b$ .

### 2.2 Fitting results

There are two results with the same fit quality. The  $\chi^2/ndf$  is  $102/45 \approx 2.3$ , where  $ndf$  is the number of degrees of freedom. Solution I corresponds to the case of constructive interference between the resonant and non-resonant contributions, and solution II corresponds to the case of destructive interference. The phase  $\phi$  and  $\Gamma_R^{e^+e^-} B_R$  are different for the two solutions. The results of the fit are displayed in Fig. 2 and Fig. 3. An obvious resonance structure is observed with mass  $M_R = (2207 \pm 14) \text{ MeV}/c^2$ , width  $\Gamma_R = (104 \pm 16) \text{ MeV}$ . According to PDG<sup>[8]</sup>, the mass of the resonance is very close to  $\omega(2205)$ , which is  $(2205 \pm 30) \text{ MeV}/c^2$ , but the width is much smaller than  $\omega(2205)$ , which is  $(350 \pm 90) \text{ MeV}$ . Compared with the individual fitting results<sup>[20–22]</sup>, the result in this paper is consistent with all of them, and very close to the average value of the three results. Details of the fit are listed in Table 1.

## 3 Simultaneous fit with two resonances

The masses of  $\omega(4S)$  and  $\omega(3D)$  are all around 2.2 GeV according to the theoretical study<sup>[9,24]</sup>, and the resonances in  $e^+e^- \rightarrow \omega\pi^0\pi^0, \pi^+\pi^-$ , and  $\omega\eta$  are contributed by  $\omega(4S)$  and  $\omega(3D)$ . This indicates that we can perform a simultaneous fit to the Born cross section line shapes of the three processes by

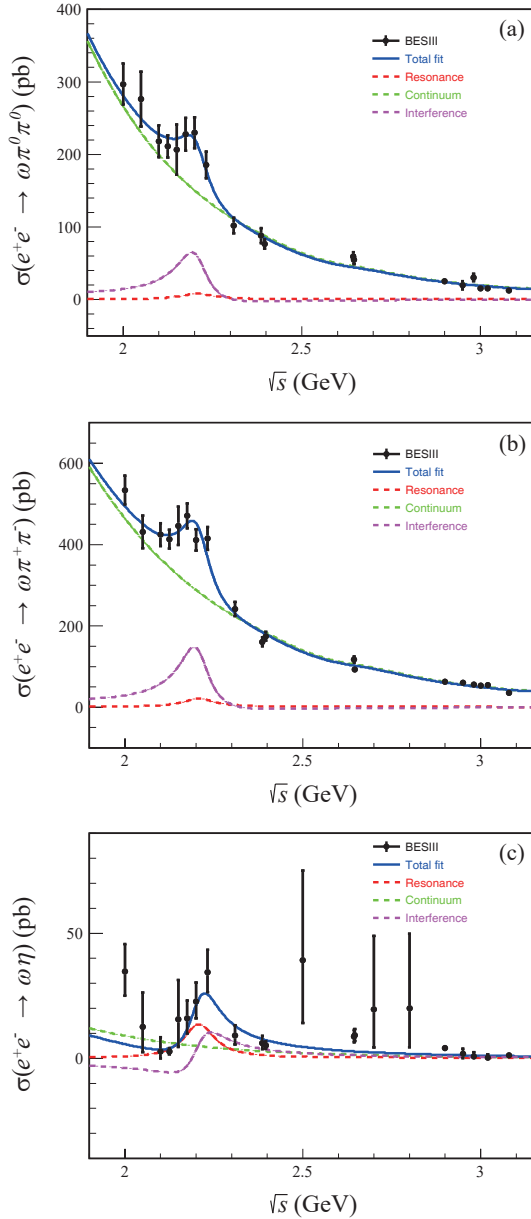


**Fig. 2.** Solution I of the simultaneous fit of  $e^+e^- \rightarrow \omega\pi^0\pi^0$ ,  $\omega\pi^+\pi^-$ , and  $\omega\eta$  with one resonance. Black dots with error bars are from experimental data, and the error bars include both statistical and systematic uncertainties. The blue solid curve represents the total fit. The red dashed curve represents the contribution of resonant part. The green dashed curve presents the contribution of non-resonant part. The pink curve represents the interference between the two parts.

adding two resonances representing  $\omega(4S)$  and  $\omega(3D)$ .

### 3.1 Fitting method

The method is the same as in Section 2, and the function is a coherent sum of two resonant contributions and a non-resonant contribution:

$$\sigma^B(\sqrt{s}) = |A_{\omega(4S)}(\sqrt{s})e^{i\phi(4S)} + A_{\omega(3D)}(\sqrt{s})e^{i\phi(3D)} + A_c(\sqrt{s})|^2, \quad (7)$$

where  $\phi(4S)$  and  $\phi(3D)$  are relative phases between the resonant and non-resonant amplitudes,  $A_{\omega(4S)}(\sqrt{s})$  and  $A_{\omega(3D)}(\sqrt{s})$  are the resonant components, which are parameterized with

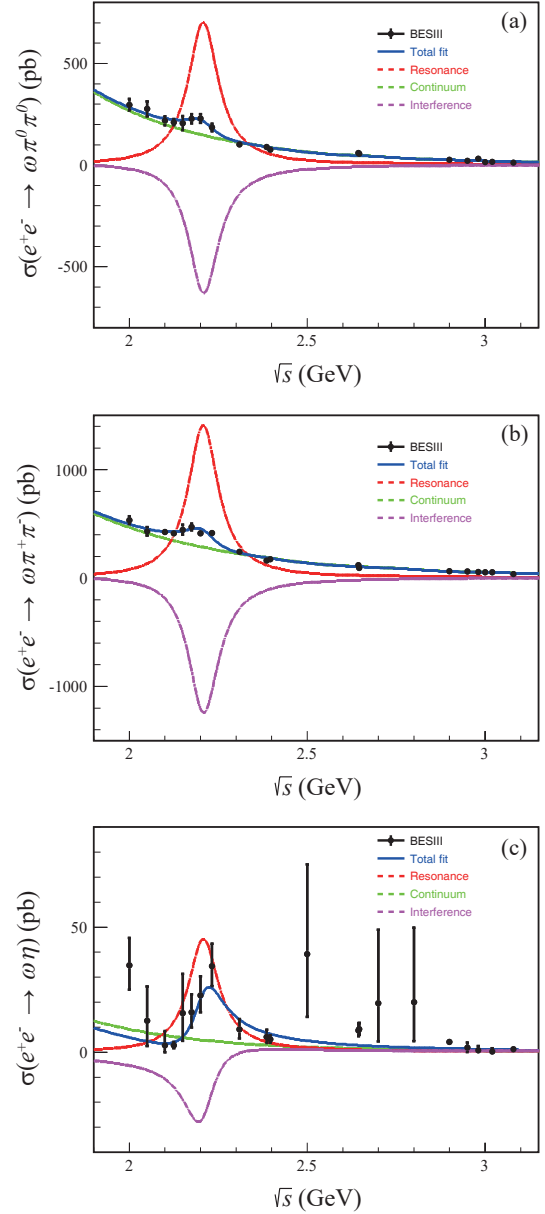


**Fig. 3.** Solution II of the simultaneous fit of  $e^+e^- \rightarrow \omega\pi^0\pi^0$ ,  $\omega\pi^+\pi^-$ , and  $\omega\eta$  with one resonance. The symbols' descriptions are consistent with Fig. 2.

the Breit-Wigner function same as in Section 2.  $A_c(\sqrt{s})$  is the non-resonant component, parameterized with the same function as in Section 2. In the simultaneous fit,  $M_R(4S)$ ,  $M_R(3D)$ ,  $\Gamma_R(4S)$ , and  $\Gamma_R(3D)$  are shared parameters, so there are 22 free parameters in total, including  $M_R(4S)$ ,  $M_R(3D)$ ,  $\Gamma_R(4S)$ ,  $\Gamma_R(3D)$ , and three sets of  $\phi(4S)$  and  $\Gamma_R^{e^+e^-} B_R(4S)$ ,  $\phi(3D)$  and  $\Gamma_R^{e^+e^-} B_R(3D)$ ,  $a$  and  $b$ .

### 3.2 Fitting results

There are two results with the same fit quality. The  $\chi^2/ndf$  is  $47/37 \approx 1.3$ , which is smaller than the previous fit. Both constructive and destructive interference between resonant and non-resonant contributions are included in solution I and solution II. The mass, width, phase  $\phi$ ,  $\Gamma_R^{e^+e^-} B_R$  are different for the two solutions. In the same solution,  $\phi$  and  $\Gamma_R^{e^+e^-} B_R$  for  $\omega(4S)$  and  $\omega(3D)$  are also different, too. In some cases, the

**Table 1.** Details for the simultaneous fit of  $e^+e^- \rightarrow \omega\pi^0\pi^0$ ,  $\omega\pi^+\pi^-$ , and  $\omega\eta$  with one resonance.

Process	Parameter	Solution I	Solution II
$\omega\pi^0\pi^0$	$M_R(\text{MeV}/c^2)$	$2207 \pm 14$	
	$\Gamma_R(\text{MeV})$	$104 \pm 16$	
	$\phi(\text{rad})$	$2.05 \pm 0.24$	$-1.72 \pm 0.02$
	$\Gamma_R^{e^+e^-} B_R(\text{eV})$	$0.27 \pm 0.12$	$24.12 \pm 0.83$
	$a(10^3\text{pb}^{1/2})$	$1.24 \pm 0.14$	$1.27 \pm 0.14$
	$b$	$4.95 \pm 0.13$	$4.99 \pm 0.13$
$\omega\pi^+\pi^-$	$\phi(\text{rad})$	$1.99 \pm 0.15$	$-1.71 \pm 0.02$
	$\Gamma_R^{e^+e^-} B_R(\text{eV})$	$0.70 \pm 0.19$	$48.43 \pm 1.13$
	$a(10^3\text{pb}^{1/2})$	$1.16 \pm 0.10$	$1.18 \pm 0.10$
	$b$	$4.45 \pm 0.09$	$4.47 \pm 0.09$
$\omega\eta$	$\phi(\text{rad})$	$0.32 \pm 0.22$	$-1.16 \pm 0.11$
	$\Gamma_R^{e^+e^-} B_R(\text{eV})$	$0.46 \pm 0.16$	$1.55 \pm 0.19$
	$a(10^3\text{pb}^{1/2})$	$0.25 \pm 0.17$	$0.28 \pm 0.15$
	$b$	$5.73 \pm 0.85$	$5.88 \pm 0.96$
	$\chi^2/\text{ndf}$	2.3	

contribution from  $\omega(4S)$  is larger than the contribution from  $\omega(3D)$ . Otherwise, it is the opposite. The results for the fits are displayed in Fig. 4 and Fig. 5. The resonant structures observed in the three processes are well described by two resonances. For  $\omega(4S)$ , the mass is around  $2160 \text{ MeV}/c^2$ , and the width is around  $150 \text{ MeV}$ . For  $\omega(3D)$ , the mass is around  $2300 \text{ MeV}/c^2$ , and the width is around  $100 \text{ MeV}$ . The theoretical prediction of  $\omega(4S)$  is  $M = 2180 \text{ MeV}/c^2$ ,  $\Gamma = 104 \text{ MeV}$ . The prediction for  $\omega(3D)$  is  $M = 2283 \text{ MeV}/c^2$ ,  $\Gamma = 94 \text{ MeV}$ <sup>[24]</sup>. The fitting results are consistent with theoretical predictions. Details of the fit are listed in Table 2.

## 4 Simultaneous fit of the intermediate processes in $e^+e^- \rightarrow \omega\pi^+\pi^-$

In the analysis of  $e^+e^- \rightarrow \omega\pi^+\pi^-$ <sup>[20]</sup>, the Born cross sections of the intermediate subprocesses are determined with the PWA method. Based on the data, we perform two simultaneous fits for the subprocesses  $e^+e^- \rightarrow \omega f_0(500)$ ,  $\omega f_0(980)$ ,  $\omega f_2(1270)$ , and  $b_1(1235)\pi$ , where the masses and widths are fixed to be the values obtained before.

### 4.1 Fitting method

For the fit with one resonance, we use the same function as Eq. (4) for each mode. The mass and width are shared parameters, and they are fixed to be the values in Table 1. There are 16 parameters in total: four sets of  $\phi$ ,  $\Gamma_R^{e^+e^-} B_R$ ,  $a$  and  $b$ .

For the fit with two resonances representing  $\omega(4S)$  and

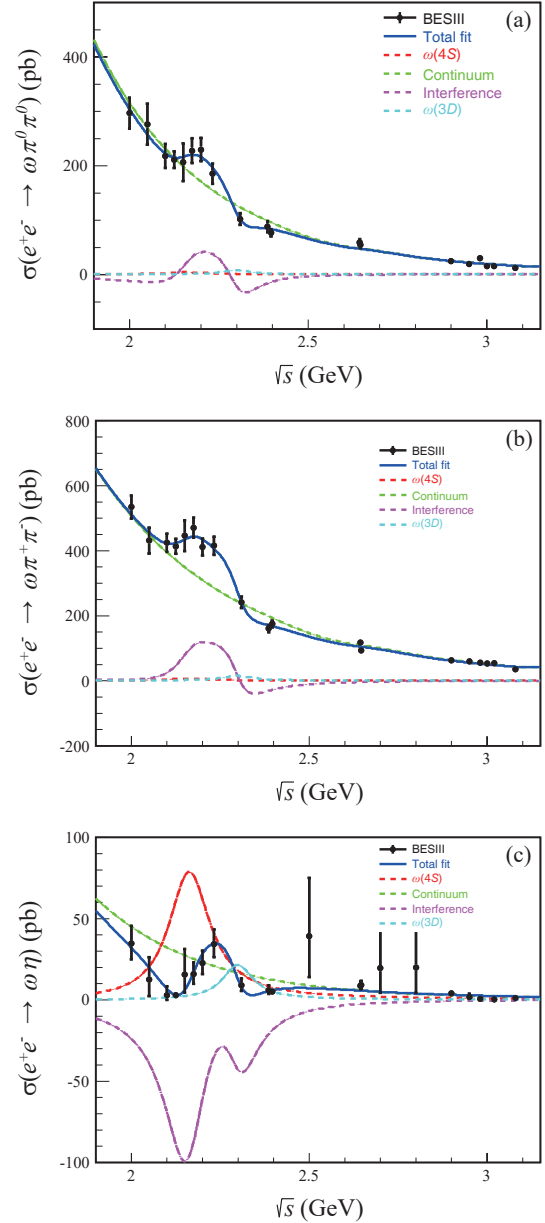


**Fig. 4.** Solution I of the simultaneous fit of  $e^+e^- \rightarrow \omega\pi^0\pi^0$ ,  $\omega\pi^+\pi^-$ , and  $\omega\eta$  with two resonances. Black dots with error bars are from experimental data, and the error bars include both statistical and systematic uncertainties. The blue solid curve represents the total fit. The red dashed curve represents the contribution of  $\omega(4S)$ . The cyan dashed curve represents the contribution of  $\omega(3D)$ . The green dashed curve presents the contribution of non-resonant part. The pink curve represents the interference between the resonant and non-resonant parts.

$\omega(3D)$ , we use the same function as Eq. (7) for each mode. The mass and width for  $\omega(4S)$  and  $\omega(3D)$  are shared parameters, and they are fixed to be the values of solution I in Table 2, as Solution I is closer to the theoretical predictions. There are 24 parameters in total: four sets of  $\phi(4S)$  and  $\Gamma_R^{e^+e^-} B_R(4S)$ ,  $\phi(3D)$  and  $\Gamma_R^{e^+e^-} B_R(3D)$ ,  $a$  and  $b$ .

### 4.2 Fitting results

For the fit with one resonance, we obtain two results with the same fit quality. The resonant structure in each mode is well described with one resonant component. The  $\chi^2/\text{ndf}$  is



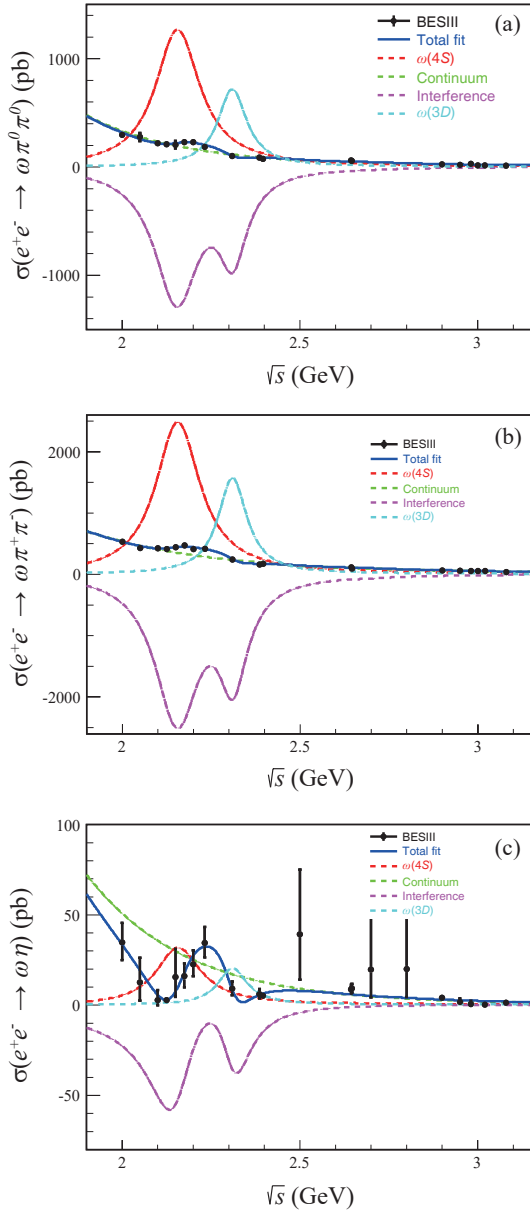


**Fig. 5.** Solution II of the simultaneous fit of  $e^+e^- \rightarrow \omega\pi^0\pi^0$ ,  $\omega\pi^+\pi^-$  and  $\omega\eta$  with two resonances. The symbols' descriptions are consistent with Fig. 4.

$39/31 \approx 1.3$ . Solution I corresponds to the case of constructive interference between the resonant and non-resonant contributions. Solution II corresponds to the case of destructive interference. The phases  $\phi$  and  $\Gamma_R^{e^+e^-} B_R$  are different for the two solutions. The results of the fits are displayed in Fig. 6 and Fig. 7. Details of the fit are listed in Table 3. The fitted  $\Gamma_R^{e^+e^-} B_R$  values are compared with the results in Ref. [20] in Table 4. The results are partially consistent with each other. The inconsistency is due to different fitting conditions.

For the fit with two resonances, we get two results with the same fit quality. The resonant structure in each mode is well described with two resonant components representing  $\omega(4S)$  and  $\omega(3D)$ . The  $\chi^2/ndf$  is  $23/23 = 1.0$ , which is smaller than the fit with one resonance. Solution I corresponds to the case of constructive interference, Solution II mostly corresponds to the case of destructive interference. The phase  $\phi(4S)$ ,  $\phi(3D)$  and  $\Gamma_R^{e^+e^-} B_R(4S)$ ,  $\Gamma_R^{e^+e^-} B_R(3D)$  are different for the two

**Table 2.** Details for the simultaneous fit of  $e^+e^- \rightarrow \omega\pi^0\pi^0$ ,  $\omega\pi^+\pi^-$ , and  $\omega\eta$  with two resonances.

Process	Parameter	Solution I	Solution II
$\omega\pi^0\pi^0$	$M_R(4S)(\text{MeV}/c^2)$	$2160 \pm 36$	$2154 \pm 12$
	$\Gamma_R(4S)(\text{MeV})$	$141 \pm 74$	$152 \pm 77$
	$M_R(3D)(\text{MeV}/c^2)$	$2298 \pm 19$	$2309 \pm 6$
	$\Gamma_R(3D)(\text{MeV})$	$106 \pm 77$	$99 \pm 23$
$\omega\pi^+\pi^-$	$\phi(4S)(\text{rad})$	$0.19 \pm 0.81$	$-1.33 \pm 0.17$
	$\Gamma_R^{e^+e^-} B_R(4S)(\text{eV})$	$0.17 \pm 0.28$	$60.68 \pm 21.79$
	$\phi(3D)(\text{rad})$	$-2.49 \pm 0.69$	$-2.86 \pm 0.39$
	$\Gamma_R^{e^+e^-} B_R(3D)(\text{eV})$	$0.27 \pm 0.23$	$25.72 \pm 7.79$
$\omega\eta$	$a(10^3\text{pb}^{1/2})$	$1.58 \pm 0.26$	$2.25 \pm 0.56$
	$b$	$5.17 \pm 0.18$	$5.65 \pm 0.32$
	$\phi(4S)(\text{rad})$	$0.59 \pm 0.66$	$-1.30 \pm 0.17$
	$\Gamma_R^{e^+e^-} B_R(4S)(\text{eV})$	$0.26 \pm 0.25$	$118.85 \pm 43.40$
$\omega\pi^+\pi^-$	$\phi(3D)(\text{rad})$	$-2.99 \pm 0.42$	$-2.84 \pm 0.37$
	$\Gamma_R^{e^+e^-} B_R(3D)(\text{eV})$	$0.51 \pm 0.27$	$56.24 \pm 27.55$
	$a(10^3\text{pb}^{1/2})$	$1.30 \pm 0.15$	$1.59 \pm 0.24$
	$b$	$4.55 \pm 0.12$	$4.81 \pm 0.18$
$\omega\eta$	$\phi(4S)(\text{rad})$	$-1.22 \pm 0.37$	$-0.96 \pm 0.13$
	$\Gamma_R^{e^+e^-} B_R(4S)(\text{eV})$	$3.51 \pm 3.05$	$1.51 \pm 0.44$
	$\phi(3D)(\text{rad})$	$3.13 \pm 0.43$	$-2.68 \pm 0.19$
	$\Gamma_R^{e^+e^-} B_R(3D)(\text{eV})$	$0.81 \pm 0.96$	$0.73 \pm 0.49$
$\omega\eta$	$a(10^3\text{pb}^{1/2})$	$0.69 \pm 0.51$	$0.86 \pm 0.34$
	$b$	$6.03 \pm 0.84$	$6.27 \pm 0.46$
$\chi^2/ndf$		1.3	

solutions. For the same solution of one mode,  $\phi$  and  $\Gamma_R^{e^+e^-} B_R$  for  $\omega(4S)$  and  $\omega(3D)$  are different, too. In most of the cases, contribution from  $\omega(4S)$  is larger than  $\omega(3D)$ . The results of the fits are displayed in Fig. 8 and Fig. 9. Details of the fit are listed in Table 5.  $\Gamma_R^{e^+e^-} B_R(4S/3D)$  of the modes  $b_1(1235)\pi$  and  $\omega f_2(1270)$  have been calculated in theory in Refs. [23, 24]. Table 6 compares the fitted results with the theoretical prediction. For the  $\omega f_2(1270)$  mode, Solution I is consistent with theory by taking the uncertainties into account. For the  $b_1(1235)\pi$  mode, the results are inconsistent between theory and experiment.

## 5 Conclusions

Inspired by the knowledge of Refs. [23, 24], we make a joint

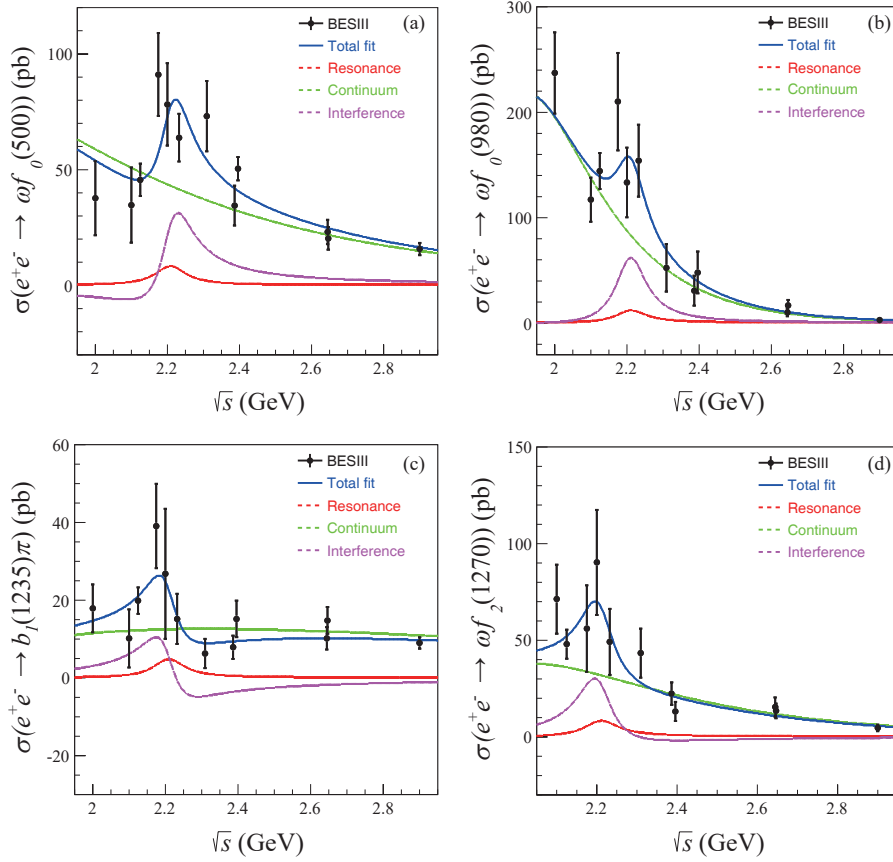


Fig. 6. Solution I of the simultaneous fit of the intermediate modes in  $e^+e^- \rightarrow \omega\pi^+\pi^-$  with one resonance. The symbol descriptions are consistent with Fig. 2.

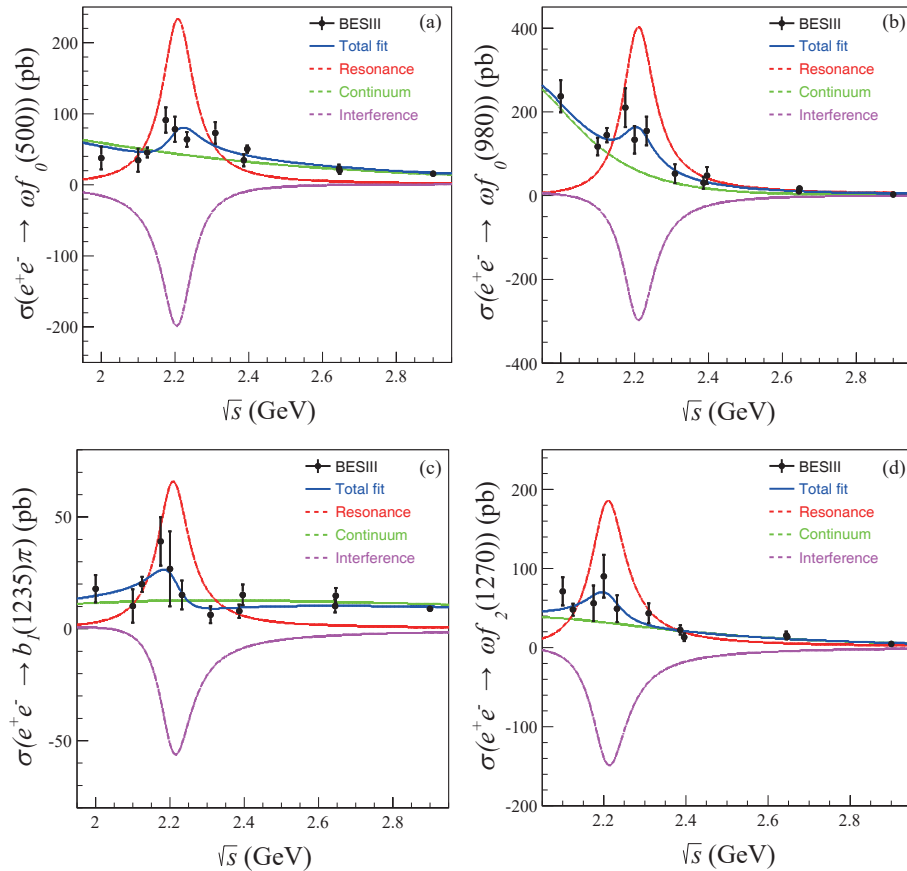


Fig. 7. Solution II of the simultaneous fit of the intermediate modes in  $e^+e^- \rightarrow \omega\pi^+\pi^-$  with one resonance. The symbol description is consistent with Fig. 2.

**Table 3.** Details for the simultaneous fit of the intermediate modes in  $e^+e^- \rightarrow \omega\pi^+\pi^-$  with one resonance.

Process	Parameter	Solution I	Solution II
$\omega f_0(500)$	$\phi(\text{rad})$	$0.74 \pm 0.34$	$-1.51 \pm 0.05$
	$\Gamma_R^{e^+e^-} B_R(\text{eV})$	$0.28 \pm 0.13$	$8.02 \pm 0.55$
	$a(10^3\text{pb}^{1/2})$	$0.19 \pm 0.06$	$0.19 \pm 0.06$
	$b$	$4.02 \pm 0.37$	$4.03 \pm 0.38$
$\omega f_0(980)$	$\phi(\text{rad})$	$1.35 \pm 0.56$	$-1.84 \pm 0.08$
	$\Gamma_R^{e^+e^-} B_R(\text{eV})$	$0.40 \pm 0.31$	$13.79 \pm 1.30$
	$a(10^3\text{pb}^{1/2})$	$34.71 \pm 24.39$	$155.28 \pm 196.18$
	$b$	$9.60 \pm 0.89$	$11.72 \pm 1.84$
$b_1(1235)\pi$	$\phi(\text{rad})$	$2.73 \pm 0.41$	$-1.86 \pm 0.09$
	$\Gamma_R^{e^+e^-} B_R(\text{eV})$	$0.16 \pm 0.11$	$2.26 \pm 0.33$
	$a(10^3\text{pb}^{1/2})$	$0.05 \pm 0.02$	$0.05 \pm 0.02$
	$b$	$2.74 \pm 0.46$	$2.74 \pm 0.46$
$\omega f_2(1270)$	$\phi(\text{rad})$	$1.81 \pm 0.44$	$-1.75 \pm 0.08$
	$\Gamma_R^{e^+e^-} B_R(\text{eV})$	$0.25 \pm 0.25$	$6.38 \pm 0.72$
	$a(10^3\text{pb}^{1/2})$	$5.60 \pm 0.75$	$0.78 \pm 0.57$
	$b$	$0.72 \pm 0.48$	$5.71 \pm 0.83$
$\chi^2/\text{ndf}$		1.3	

**Table 4.** Comparison of  $\Gamma_R^{e^+e^-} B_R$  of the intermediate modes in  $e^+e^- \rightarrow \omega\pi^+\pi^-$  between fitted results and Ref. [20].

Process	This work		Ref. [20]	
	Solution I	Solution II	Solution I	Solution II
$\omega f_0(500)$	$0.28 \pm 0.13$	$8.02 \pm 0.55$	$2.9 \pm 2.5$	$1.2 \pm 0.5$
$\omega f_0(980)$	$0.40 \pm 0.31$	$13.79 \pm 1.30$	$5.9 \pm 5.0$	$3.2 \pm 1.0$
$b_1(1235)\pi$	$0.16 \pm 0.11$	$2.26 \pm 0.33$	$1.1 \pm 1.0$	$0.2 \pm 0.2$
$\omega f_2(1270)$	$0.25 \pm 0.25$	$6.38 \pm 0.72$	$2.5 \pm 2.1$	$1.1 \pm 0.6$

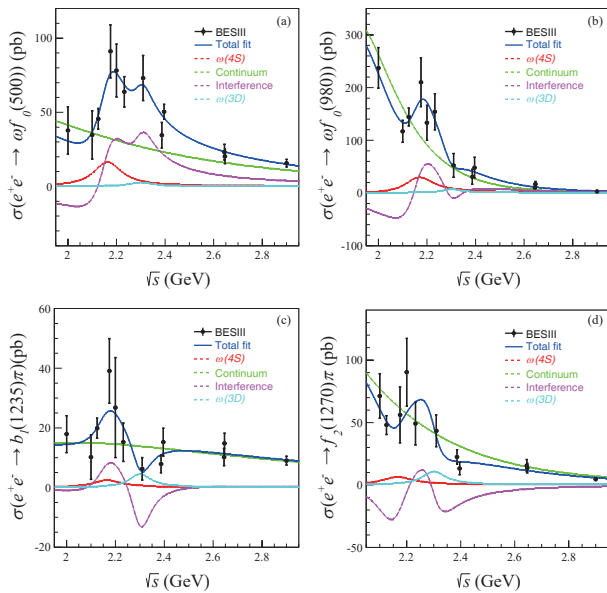


**Fig. 8.** Solution I of the simultaneous fit of the intermediate modes in  $e^+e^- \rightarrow \omega\pi^+\pi^-$  with two resonances. The symbols' descriptions are consistent with Fig. 4

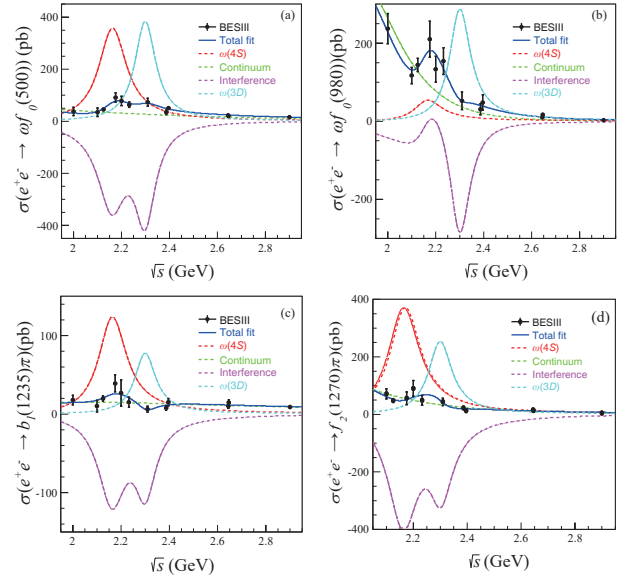


**Fig. 9.** Solution II of the simultaneous fit of the intermediate modes in  $e^+e^- \rightarrow \omega\pi^+\pi^-$  with two resonances. The symbols' descriptions are consistent with Fig. 4.

**Table 5.** Details for the simultaneous fit of the intermediate modes in  $e^+e^- \rightarrow \omega\pi^+\pi^-$  with two resonances.

Process	Parameter	Solution I	Solution II
$\omega f_0(500)$	$\phi(4S)(\text{rad})$	$0.47 \pm 0.31$	$-0.86 \pm 0.13$
	$\Gamma_R^{e^+e^-} B_R(4S)(\text{eV})$	$0.72 \pm 0.52$	$15.94 \pm 1.86$
	$\phi(3D)(\text{rad})$	$0.76 \pm 0.91$	$-2.54 \pm 0.08$
	$\Gamma_R^{e^+e^-} B_R(3D)(\text{eV})$	$0.10 \pm 0.69$	$14.57 \pm 1.44$
$\omega f_0(980)$	$a(10^3\text{pb}^{1/2})$	$0.15 \pm 0.11$	$0.16 \pm 0.12$
	$b$	$3.95 \pm 0.72$	$4.00 \pm 0.78$
	$\phi(4S)(\text{rad})$	$0.25 \pm 0.36$	$0.56 \pm 0.28$
	$\Gamma_R^{e^+e^-} B_R(4S)(\text{eV})$	$1.30 \pm 1.24$	$2.34 \pm 2.06$
$b_1(1235)\pi$	$\phi(3D)(\text{rad})$	$-1.91 \pm 1.13$	$-1.78 \pm 0.21$
	$\Gamma_R^{e^+e^-} B_R(3D)(\text{eV})$	$0.24 \pm 0.36$	$10.90 \pm 1.81$
	$a(10^3\text{pb}^{1/2})$	$102.81 \pm 133.83$	$192.34 \pm 261.15$
	$b$	$10.95 \pm 1.87$	$11.85 \pm 2.09$
$\omega f_2(1270)$	$\phi(4S)(\text{rad})$	$0.95 \pm 0.68$	$-1.15 \pm 0.11$
	$\Gamma_R^{e^+e^-} B_R(4S)(\text{eV})$	$0.11 \pm 0.16$	$5.50 \pm 0.74$
	$\phi(3D)(\text{rad})$	$-1.78 \pm 0.49$	$-2.71 \pm 0.10$
	$\Gamma_R^{e^+e^-} B_R(3D)(\text{eV})$	$0.17 \pm 0.18$	$2.93 \pm 0.70$
$\omega f_2(1270)$	$a(10^3\text{pb}^{1/2})$	$0.08 \pm 0.06$	$0.09 \pm 0.06$
	$b$	$3.39 \pm 0.65$	$3.40 \pm 0.66$
	$\phi(4S)(\text{rad})$	$-1.17 \pm 0.65$	$-1.37 \pm 0.08$
	$\Gamma_R^{e^+e^-} B_R(4S)(\text{eV})$	$0.28 \pm 0.63$	$16.51 \pm 2.14$
$\omega f_2(1270)$	$\phi(3D)(\text{rad})$	$3.05 \pm 0.44$	$-3.08 \pm 0.09$
	$\Gamma_R^{e^+e^-} B_R(3D)(\text{eV})$	$0.40 \pm 0.37$	$9.60 \pm 1.38$
	$a(10^3\text{pb}^{1/2})$	$1.74 \pm 1.58$	$3.11 \pm 5.09$
	$b$	$6.35 \pm 0.94$	$7.20 \pm 1.91$
$\chi^2/\text{ndf}$		1.0	



**Table 6.** Comparison of  $\Gamma_R^{e^+e^-} B_R(4S/3D)$  of the modes  $b_1(1235)\pi$  and  $\omega f_2(1270)$  between fitted results and theoretical prediction.

Process	Parameter	Solution I	Solution II	Theory
$b_1(1235)\pi$	$\Gamma_R^{e^+e^-} B_R(4S)(\text{eV})$	$0.11 \pm 0.16$	$5.50 \pm 0.74$	0.875
	$\Gamma_R^{e^+e^-} B_R(3D)(\text{eV})$	$0.17 \pm 0.18$	$2.93 \pm 0.70$	0.632
$\omega f_2(1270)$	$\Gamma_R^{e^+e^-} B_R(4S)(\text{eV})$	$0.28 \pm 0.63$	$16.51 \pm 2.14$	0.081
	$\Gamma_R^{e^+e^-} B_R(3D)(\text{eV})$	$0.40 \pm 0.37$	$9.60 \pm 1.38$	0.042

analysis of the data of  $e^+e^- \rightarrow \omega\pi^0\pi^{0[21]}$ ,  $e^+e^- \rightarrow \omega\pi^+\pi^{-[20]}$ , and  $e^+e^- \rightarrow \omega\eta^{[22]}$  carried out by simultaneous fits. In the simultaneous fits with one resonance, we observe a resonance structure with mass around 2.2 GeV, and width around 100 MeV. The mass is close to the PDG value of  $\omega(2205)$ , but the width is much smaller. In the simultaneous fits with two resonances, the resonance parameters of the resonances representing  $\omega(4S)$  and  $\omega(3D)$  are consistent with theoretical predictions. For  $\omega(4S)$ , the fitted mass is around 2160 MeV/ $c^2$ , and the fitted width is around 150 MeV. For  $\omega(3D)$ , the fitted mass is around 2300 MeV/ $c^2$ , and the fitted width is around 100 MeV. This supports the previous conclusion that the resonances in these processes are contributed by both  $\omega(4S)$  and  $\omega(3D)^{[23]}$ . Based on the resonance parameters, we also perform two simultaneous fits of the intermediate subprocesses in  $e^+e^- \rightarrow \omega\pi^+\pi^-$ , and the theoretical models describe the data well. The fitted  $\Gamma_R^{e^+e^-} B_R$  values are partially consistent with previous measurement<sup>[20]</sup> and theoretical prediction<sup>[23,24]</sup>.

This work is a successful application of the joint analysis method. The conclusion verifies the previous study results, and the method is hopefully useful for more analyses.

## Acknowledgements

This work was supported by the National Natural Science Foundation of China (12035013), Joint Large-Scale Scientific Facility Funds (U1732263), and National Key R&D Program of China (2020YFA0406403).

## Conflict of interest

The authors declare that they have no conflict of interest.

## Biographies

**Yan Wu** is currently pursuing his master's degree in Department of Modern Physics at University of Science and Technology of China. His primary research is related with experimental high energy physics at BESIII.

**Qinsong Zhou** is currently pursuing his Ph.D. degree in School of Physical Science and Technology at Lanzhou University. His primary research is related with theoretical high energy physics. He has published several papers at *Physical Review C*, *Physical Review D*, and *The European Physical Journal C*.

## References

- Wang J Z, Chen D Y, Liu X, et al. Costructing  $J/\psi$  family with updated data of charmoniumlike  $Y$  states. *Phys. Rev. D*, **2019**, *99* (11): 114003.
- Wang J Z, Qian R Q, Liu X, et al. Are the  $Y$  states around 4.6 GeV from  $e^+e^-$  annihilation higher charmonia? *Physical Review D*, **2020**, *101*: 034001.
- Wang J Z, Sun Z F, Liu X, et al. Higher bottomonium zoo. *The European Physical Journal C*, **2018**, *78* (11): 915.
- Pang C Q, Wang J Z, Liu X, et al. A systematic study of mass spectra and strong decay of strange mesons. *The European Physical Journal C*, **2017**, *77* (12): 861.
- Song Q T, Chen D Y, Liu X, et al. Charmed-strange mesons revisited: Mass spectra and strong decays. *Physical Review D*, **2015**, *91*: 054031.
- Song Q T, Chen D Y, Liu X, et al. Higher radial and orbital excitations in the charmed meson family. *Physical Review D*, **2015**, *92*: 074011.
- Wang J Z, Chen D Y, Song Q T, et al. Revealing the inner structure of the newly observed  $D_2^*(3000)$ . *Physical Review D*, **2016**, *94*: 094044.
- Particle Data Group, R. L. Workman R L, Burkert V D, et al. Review of particle physics. *Progress of Theoretical and Experimental Physics*, **2022**, *8*: 083C01.
- Pang C Q, Wang Y R, Hu J F, et al. Study of the  $\omega$  meson family and newly observed  $\omega$ -like state X(2240). *Physical Review D*, **2020**, *101*: 074022.
- Barnes T, Close F E, Page P R, et al. Higher quarkonia. *Physical Review D*, **1997**, *55*: 4157–4188.
- Ebert D, Faustov R N, Galkin V O. Masses of light mesons in the relativistic quark model. *Modern Physics Letters A*, **2005**, *20*: 1887–1893.
- Ebert D, Faustov R N, Galkin V O. Mass spectra and Regge trajectories of light mesons in the relativistic quark model. *Physical Review D*, **2009**, *79*: 114029.
- Wang X, Sun Z F, Chen D Y, et al. Nonstrange partner of strangeonium-like state  $Y(2175)$ . *Physical Review D*, **2012**, *85*: 074024.
- Anisovich A V, Baker C A, Batty C J, et al.  $I=0, C=-1$  mesons from 1940 to 2410 MeV. *Physics Letters B*, **2002**, *542*: 19–28.
- Bugg D V. Partial wave analysis of  $\bar{p}p \rightarrow \bar{\Lambda}\Lambda$ . *The European Physical Journal C-Particles and Fields*, **2004**, *36*: 161–168.
- Omega Photon Collaboration, Atkinson M, Axon T J, et al. Photon diffractive dissociation to  $\rho\rho\pi$  and  $\rho\pi\pi$  states. *Zeitschrift für Physik C Particles and Fields*, **1988**, *38*: 535–541.
- Aubert B, Bona M, Boutigny D, et al. The  $e^+e^- \rightarrow 2(\pi^+\pi^-)\pi^0, 2(\pi^-\pi^+)\eta, K^+K^-\pi^+\pi^0$  and  $K^+K^-\pi^-\pi^0$  cross sections measured with initial-state radiation. *Physical Review D*, **2007**, *76*: 092005.
- Lees J P, Poireau V, Tisserand V, et al. Study of the reactions  $e^+e^- \rightarrow \pi^+\pi^-\pi^0\pi^0$  and  $\pi^+\pi^-\pi^0\pi^0\eta$  at center-of-mass energies from threshold to 4.35 GeV using initial-state radiation. *Physical Review D*, **2018**, *98*: 112015.
- Lees J P, Poireau V, Tisserand V, et al. Resonances in  $e^+e^-$  annihilation near 2.2 GeV. *Physical Review D*, **2020**, *101*: 012011.

- [20] The BESIII collaboration, Ablikim M, Achasov M N, et al. Measurement of  $e^+e^- \rightarrow \omega\pi^+\pi^-$  cross section at  $\sqrt{s} = 2.000$  to  $3.080$  GeV. *Journal of High Energy Physics*, **2023**, *1*: 111.
- [21] M. Ablikim, Achasov M N, Adlarson P, et al. Measurement of the  $e^+e^- \rightarrow \omega\pi^0\pi^0$  cross section at center-of-mass energies from  $2.0$  to  $3.08$  GeV. *Physical Review D*, **2022**, *105*: 032005.
- [22] Ablikim M, Achasov M N, Adlarson P, et al. Observation of a resonant structure in  $e^+e^- \rightarrow \omega\eta$  and another in  $e^+e^- \rightarrow \omega\pi^0$  at center-of-mass energies between  $2.00$  GeV and  $3.08$  GeV. *Physics Letters B*, **2021**, *813*: 136059.
- [23] Zhou Q S, Wang J Z, Liu X. Role of the  $\omega(4S)$  and  $\omega(3D)$  states in mediating the  $e^+e^- \rightarrow \omega\eta$  and  $\omega\pi^0\pi^0$  processes. *Physical Review D*, **2022**, *106*: 034010.
- [24] Wang J Z, Wang L M, Liu X, et al. Deciphering the light vector meson contribution to the cross sections of  $e^+e^-$  annihilations into the open-strange channels through a combined analysis. *Physical Review D*, **2021**, *104*: 054045.